

1 Introduction

Polyaromatic hydrocarbons (PAHs) refer to a group of compounds that multiple aromatic rings are fused together, such as naphthalene (2 rings), phenanthrene and anthracene (3 rings), fluoranthene and pyrene (4 rings) and benzo[a]pyrene (5 rings) and so on. These PAHs have both natural and anthropogenic occurrences. The existence of natural PAHs was always concomitant with formation of crude oil, volcanic eruption and forest fire. As for the anthropogenic PAHs, they mainly resulted from the incomplete combustion of fossil fuel by human activities (Stone et al., 2007), and heavily threaten public health (Zhang et al., 2009). It's well-known that high-molecular-weight (HMW) PAHs were carcinogenic (Boström et al., 2002), like benzo[a]pyrene has been listed as a direct carcinogen by FDA. In addition, PAHs can accumulate in bodies, thus laying a potential and chronic risk. Because of the above properties, PAHs are listed as one of Persistent Organic Pollutants (POPs).

Biodegradation is one of the most important ways to eliminate the PAHs pollution existing in the environment (Xu and Zhou, 2017). Although PAHs were hardly metabolized by microbes because of their chemical inertia and strong hydrophobicity, some specific bacteria endowed with capability of degrading HMW PAHs have been isolated and cultured in laboratories during the past decades, such as *Mycobacterium* sp. strain. BB1 (Boldrin et al., 1993), *Mycobacterium flavescens* (Dean-Ross and Cerniglia, 1996) and *Mycobacterium* sp. strain RJGII-135 (Schneider et al., 1996). The putative metabolic pathways of PAHs employed by these microbes were proposed as follows: a dioxygen was incorporated into the substrate to form a *cis*-dihydrodiol product, then followed by reactions of dehydrogenation, ring cleavage, side-chain truncation and so on to reduce the number of rings of PAHs, and finally the intermediates entered into TCA cycles (Kweon et al., 2011). However, a complete degradation pathway at the biochemical levels hasn't been identified.

Mycobacteria vanbaalenii PYR-1 was isolated from an oil-contaminated estuary of the Gulf of Mexico using pyrene as the sole carbon source (Heitkamp et al., 1988).

The most incredible feature of this strain is that it is powerful to degrade a wide range of PAHs, including HMW PAHs with four or more fused benzene rings, such as benzo[a]pyrene (Moody et al., 2004), pyrene (Kim et al., 2007) and fluoranthene (Kweon et al., 2007), and also low-molecular-weight (LMW) PAHs like naphthalene, fluorene, phenanthrene and anthracene (Moody et al., 2001). During the PAHs degradation, the first step was catalyzed by a ring-hydroxylation dioxygenase, termed as Rieske non-heme iron-dependent oxygenase (Barry and Challis, 2013), consisting of an electron transport chain and a terminal dioxygenase. The catalytic mechanism of reaction cycle of ring-hydroxylating dioxygenase is shown in Fig. 1.

Gene *nidA3B3* (GenBank accession number: DQ028634.1) from strain PYR-1 was first reported in 2006 to incorporate a dioxygen to PAHs with its remarkable feature that it preferred HMW PAHs including fluoranthene and pyrene to LMW PAHs (Kim et al., 2006), so it was assumed that NidA3B3 maybe have a large active site (Kweon et al., 2010). In addition, only when equipped with PhdCD, an exogenous electron transport chain components of phenanthrene dioxygenase from *Nocardioides* sp. KP7 (Saito et al., 2000), NidA3B3 displayed the activity in *E. coli* (Kim et al., 2006). But NidAB (AF249301.2 and AF249302.1), the isoenzyme of NidA3B3 from the same strain, exhibited its activity without an exogenous redox partner in *E. coli* (Khan et al., 2001), which means NidAB can borrow electrons from some unknown donors in *E. coli*. Due to its important role in the catabolism of pyrene (Kim et al., 2007) and fluoranthene (Kweon et al., 2007), *nidA3B3* has been widely employed in ecological studies as a probe to detect *nidA3B3*-like dioxygenase genes involved in PAHs degradation (Zhou et al., 2006; Cébron et al., 2008). In this study, we report that NidA3B3, equipped with PhtAcAd (AAQ91918.1 and AAQ91919.1) rather than PhdCD (BAA84714.1 and BAA84715.1), an endogenous electron transport chain from a phthalate dioxygenase system, exhibited an increased activity. A newly defined protein, FNidA3B3, with a prolonged sequence of 19 amino acids (MSAHVLGAQIDRKVRPVDS) at the N-

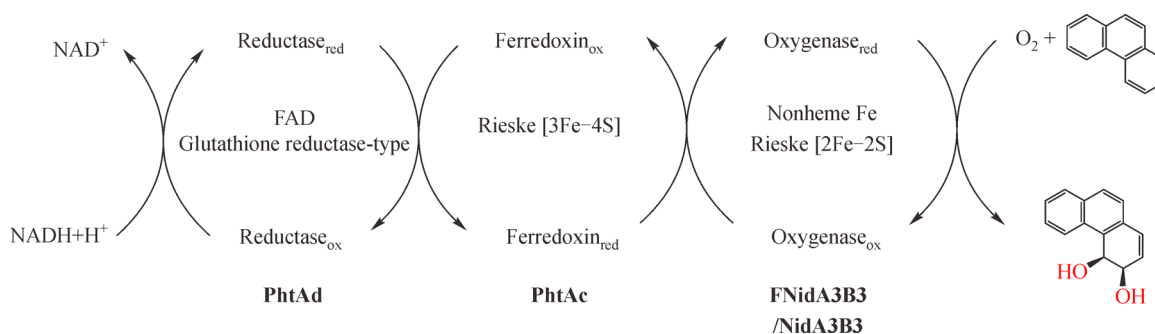


Fig. 1 Schema of a catalytic cycle by FNidA3B3/NidA3B3-PhtAcAd. A molecule of dioxygen is incorporated into PAHs with the aid of two electrons provided by NADH.

terminus of NidA3B3, also endowed a largely increased activity compared with NidA3B3. The components of electron transport chain PhtAc and PhtAd were purified and characterized. The genetic and evolutionary relationships between isoenzymes NidA3/FNidA3 and NidA from strain PYR-1 were also proposed. This research will advance our knowledge of ring-hydroxylating dioxygenases involved in microbial degradation of PAHs and maybe also contribute to our further investigation at biochemical levels thoroughly.

2 Materials and methods

2.1 Materials

2.1.1 Strains, plasmids and primers

All strains and plasmids were shown in Table 1. *M.*

vanbaalenii PYR-1 (DSM No. 7251) was purchased from Leibniz-Institut DSMZ (Germany); *E. coli* T1 and BL21 (DE3) were used as cloning and expression hosts, respectively; plasmid pETDuet-1 was used as the expression vector. And all primers were listed in Table 2.

2.1.2 Media, buffers and antibiotics

M7H10 medium containing 10% OADC growth supplement was used to cultivate *M. vanbaalenii* PYR-1 on the plate. M7H10 medium per 900 mL contains: 0.5 g (NH₄)₂SO₄, 1.5 g KH₂PO₄, 1.5 g Na₂HPO₄, 0.4 g sodium citrate, 25 mg MgSO₄, 0.5 mg CaCl₂, 1 mg ZnSO₄, 1 mg CuSO₄, 0.5 g L-sodium glutamate, 40 mg ammonium ferric citrate, 1 mg pyridoxine hydrochloride, 0.5 mg biotin, 250 g malachite green, 5 mL glycol, 15 g agar; M7H9 medium, using for liquid cultivation, per 900 mL contains: 0.5 g (NH₄)₂SO₄, 2.5 g Na₂HPO₄, 1 g KH₂PO₄, 0.1 g sodium citrate, 50 mg MgSO₄, 0.5 mg CaCl₂, 1 mg

Table 1 Strains and plasmids used in the experiment

Strains /Plasmids	Characteristics	Source
Strains		
<i>Mycobacterium vanbaalenii</i> PYR-1	Wild type; PAHs degradation bacterium	Leibniz-Institut DSMZ (Germany)
<i>E. coli</i> BL21 (DE3)	F ⁻ <i>ompT hsdSB (R^b-m^B-)</i> <i>gal (c I857 ind1 Sam7 nin5 lacUV5 T7gene1) dcm</i> (DE3)	Novagen
<i>E. coli</i> T1	F ⁻ 80 <i>lacZM15 (lacZYA-argF)U169 recA1 endA1 hsdR17(r^k-, m^k+) phoA supE44 l-thi-1 gyrA96 relA1 tonA</i>	Novagen
Plasmids		
pETDuet-1	Amp ^r , co-expression vector	Novagen
pFNidA3B3	<i>fnidA3B3</i> cloned into pETDuet-1	This study
pNidA3B3	<i>nidA3B3</i> cloned into pETDuet-1	This study
pFNidA3B3-PhtAcAd	<i>fnidA3B3</i> and <i>phtAcAd</i> cloned into pETDuet-1	This study
pNidA3B3-PhtAcAd	<i>nidA3B3</i> and <i>phtAcAd</i> cloned into pETDuet-1	This study
pNidA3B3-PhdCD	<i>nidA3B3</i> and <i>phdCD</i> cloned into pETDuet-1	This study
pPhtAc(His)	<i>phtAc</i> cloned into pETDuet-1 with His tag	This study
pPhtAd(His)	<i>phtAd</i> cloned into pETDuet-1 with His tag	This study

Table 2 Primers of PCR used in the experiment

Primers	Sequences ^{a)}
<i>fnidA3</i> (Nco I)-F	<i>TAAGAAGGAGATATACCATGGGCATGAGTGCTCACGTTCT</i>
<i>nidB3</i> (BamH I)-R	<i>GCCGAGCTCGAATTCGGATCCTTAGATCCAGAATGACAG</i>
<i>nidA3</i> (Nco I)-F	<i>TAAGAAGGAGATATACCATGGGCATGGCGCCTGATGCGA</i>
<i>phtAc</i> (Nde I)-F	<i>TAAGAAGGAGATATACATATGATGGGCGGAGTTATAAAG</i>
<i>phtAd</i> (Kpn I)-R	<i>TTTACCAGACTCGAGGGTACCCTATGGTGATCGCGTTGC</i>
<i>phtAc</i> (BamH I)-F	<i>TCATCACCCAGCCAGGATCCGATGGGCGGAGTTATAAA</i>
<i>phtAc</i> (Hind III)-R	<i>GCATTATGCGGCCGCAAGCTTTCATTCGTCTACGACTTC</i>
<i>phtAd</i> (BamH I)-F	<i>TCATCACCCAGCCAGGATCCGATGACGTGCGGGTTCGT</i>
<i>phtAd</i> (Hind III)-R	<i>GCATTATGCGGCCGCAAGCTTCTATGGTGATCGCGTTGC</i>
<i>pNidA3</i> (BamH I)-F	<i>TCATCACCCAGCCAGGATCCGATGAGTGCTCACGTTCT</i>

Note: a) The homologous sequences of pETDuet-1 are italic, the restriction sites are underlined and italic.

ZnSO₄, 1 mg CuSO₄, 40 mg ammonium ferric citrate, 0.5 g L-sodium glutamate, 1 mg pyridoxine hydrochloride, 0.5 mg biotin, 0.5 g Tween 90; OADC growth supplement per 100 mL contains: 0.85 g NaCl, 2 g dextrose, 5 g bovine serum albumin, 30 mg catalase, 60 L oleic acid. M7H10 and M7H9 media were sterilized by high-pressure-steam sterilizing, and OADC growth supplement was sterilized by filtration using 0.22 µm filter. Ampicillin was added with the concentration of 100 mg/L when necessary. For protein purification, buffer A contains: 25 mM Tris-HCl, 300 mM NaCl, 10 mM imidazole, 10% glycerol, pH = 8.0. Buffer B contains: 25 mM Tris-HCl, 300 mM NaCl, 400 mM imidazole, 10% glycerol, pH = 8.0.

2.1.3 Chemicals

Restriction enzymes were purchased from New England Biolabs (Beijing, China); high-fidelity PCR polymerase and Exnase for DNA seamless cloning were purchased from Vazyme Biotech Co. Ltd. (Nanjing, China); plasmid extraction, DNA gel extraction kits and genome extraction kits were purchased from Omega Bio-tek, Inc. (Doraville, GA, USA); Bradford Protein Assay Kit was purchased from Beyotime Institute of Biotechnology (Beijing, China); PAHs were purchased from Aladdin Bio-Chem Technology Co., Ltd (Shanghai, China); derivatization agent BSTFA-TMCS was purchased from Sigma-Aldrich Co. (St. Louis, MO, USA).

2.2 Methods

2.2.1 Cultivation, phenotype validation and genome extraction of *M. vanbaalenii* PYR-1

M. vanbaalenii PYR-1 lyophilized powder was dissolved in M7H9 medium, then was inoculated into M7H10 plate with 10% OADC. After cultivation at 30°C in dark for 7 days, single bright yellow colonies formed on the plate. A colony was inoculated into M7H9 medium with 10% OADC and 10 mg/mL PAHs, cultivated at 30°C, 160 r/min. After the growth reached stationary phase, its genome was extracted according to the manual.

2.2.2 Genes amplification and plasmids construction

Three pairs of primers *fnidA3* (NcoI)-F/*fnidB3* (BamH I)-R, *nidA3* (Nco I)-F/*nidB3* (BamH I)-R and *phtAc* (Nde I)-F/*phtAd* (Kpn I)-R (Table 2), were used to amplify genes *fnidA3B3*, *nidA3B3* and *phtAcAd* (GenBank accession number: AY365117.2), respectively, from the genomic DNA of strain PYR-1. All PCR amplified fragments were sequenced by Tsingke Biological Technology Co., Ltd. (Shanghai, China) to confirm without mutations. After

then, the two PCR products *fnidA3B3* and *nidA3B3* were individually inserted into pETDuet-1 to result in plasmids pFNidA3B3 and pNidA3B3 (Table 1). And *phtAcAd* was inserted into both pFNidA3B3 and pNidA3B3 to get the plasmids pFNidA3B3-PhtAcAd and pNidA3B3-PhtAcAd (Table 1). *phdCD* (GenBank accession number: AB017795.1) was synthesized by Personal Biotechnology Co., Ltd. (Shanghai, China), and directly inserted pNidA3B3 to get plasmid pNidA3B3-PhdCD. Two pairs of primers *phtAc*(BamH I)-F/*phtAc*(Hind III)-R and *phtAd* (BamH I)-F/*phtAd*(Hind III)-R were used to amplify genes *phtAc* and *phtAd*, respectively. After being sequenced to confirm without mutations, *phtAc* and *phtAd* were inserted in pETDuet-1 respectively to result in pPhtAc(His) and pPhtAd(His). All constructed plasmids pFNidA3B3-PhtAcAd, pNidA3B3-PhtAcAd, pNidA3B3-PhdCD, pPhtAc(His) and pPhtAd(His) were introduced into *E. coli* BL21 (DE3) for expression.

2.2.3 Biotransformation

E. coli BL21(DE3) harboring pNidA3B3-PhtAcAd, pFNidA3B3-PhtAcAd, pNidA3B3-PhdCD were cultivated in 500 mL LB containing 100 mg/L ampicillin at 37°C, 200 r/min to an OD₆₀₀ of 0.5, respectively. The cultures were then added with 0.5 mM IPTG and inoculated at 30°C for further 4 h. Cells were then harvested and washed twice with M9 minimal medium before they were individually resuspended in 30 mL M9 minimal medium with 0.1 mM or 25 µM phenanthrene, and cultivated at 37°C, 200 r/min. Five milliliter sample was taken every hour in turn. Equivalent volume ethyl acetate was used to extract the samples twice, and then the extracts for one sample was conflated. Ethyl acetate was removed by evaporation and the pellets were directly dissolved in BSTFA-TMCS, analyzed by GC-MS (GC-QQQMS TSQ8000, Thermo) after incubation at 60°C for 30 min. The specific activity of biotransformation was measured as the previous study, and 1 unit of biotransformation activity was defined as the dry weight of resting cell required to convert 1 nmol phenanthrene per minute (Wang et al., 2019).

2.2.4 GC-MS analysis

The pellets dissolved in BSTFA-TMCS were analyzed by GC-MS as following. Chromatograph condition: HP-5MS (30 m × 0.25 mm × 0.25µm) column, nitrogen as carrier gas, rate of 1 mL/min; injector temperature of 250°C. Column temperature condition: initial temperature of 60°C for 1 min, increasing to 260°C at the rate of 10°C/min, then keeping for 5min, finally increasing to 300°C at the rate of 25°C/min, keeping for 2 min. Mass spectra condition: EI ion source, electron energy of 70 eV, full scan.

2.2.5 Purification of components of electron transport chain PhtAcAd

E. coli strains, BL21(DE3) [pPhtAc (His)] and BL21(DE3) [pPhtAd (His)] were inoculated into 1 L LB and grown to an OD₆₀₀ of 0.5, respectively. Then the cultures were incubated at 16°C for 18 h after adding a final concentration of 0.5 mM IPTG. The two cultures were separately harvested and washed twice with Buffer A. The cells were separately resuspended in 60 mL Buffer A with 30 mL lysozyme, and disrupted by ultrasonication before being centrifuged at 10,000 *g* for 60 min. The supernatants were filtered through 0.45 μm filter before purification by Ni column using ÄKTA start chromatography system (GE Healthcare). The concentration of proteins were determined by BCA Protein Assay Kit.

2.2.6 Dynamic analysis of the ferredoxin reductase PhtAd and ferredoxin PhtAc

As a type of redox dye, 2,6-dichlorophenolindophenol (DCPIP) is blue when oxidized; after reduction, it turns colorless. According to this property, DCPIP could be used as an electron acceptor to determine the activity of PhtAd (Fischer et al., 2002). The reaction mixtures were 500 μL 100 mM HEPES buffer (pH = 7.5) containing 39 pmol PhtAd, 0.5 μM FAD, 30 μM DCPIP and 40 μM–250 μM NADH, and the reaction was monitored at 600nm by a Lambda 25 UV/VIS Spectrometer ($\epsilon_{600\text{nm}}$ of DCPIP is 23 mM⁻¹·cm⁻¹). The absorbance at 550 nm of cytochrome *c* increases after accepting an electron, so it could be used to determine the couple of ferredoxin PhtAc with the ferredoxin reductase PhtAd (McLean et al., 2006). The reaction mixtures were 500 μL 100 mM HEPES buffer (pH = 7.5) containing 39 pmol PhtAd, 158 pmol PhtAc, 0.5 μM FAD, 600 μM cytochrome *c* and 20 μM–400 μM NADH, and the reaction was monitored at 550 nm by a Lambda 25 UV/VIS Spectrometer ($\epsilon_{550\text{nm}}$ of cytochrome *c* is 21 mM⁻¹·cm⁻¹).

3 Results

3.1 Strain PYR-1 harbors the ability to utilize PAHs

To confirm that the strain purchased from DSMZ still harbors the ability to degrade PAHs, strain PYR-1 was inoculated to M7H9 medium containing 10% OADC supplemented with 10 mg/mL four different PAHs, respectively. During the process of metabolism of PAHs in strain PYR-1, some colorful metabolites were produced resulting in a series of color changes (Kweon et al., 2014), thus the degradation of PAHs could be easily and directly validated.

After inoculation for seven days, single and round bright

yellow colonies grew up on the M7H10 medium plate containing 10% OADC growth supplement from lyophilized powder of strain PYR-1 cells. In the area congested with colonies, abundant viscous substance was excreted and linked together into a stretch. Some colonies first appeared pink, then gradually turned yellow. All these morphologically different colonies have been validated to belong to *M. vanbaalenii* by 16S rRNA gene sequencing. The morphological changes indicated that strain PYR-1 possesses a powerful system to produce pigments and it may be tightly regulated.

Strain PYR-1 was able to grow in the liquid M7H9 medium with 10% OADC growth supplement with different PAHs, respectively. After 17 h incubation, the medium containing fluorene turned yellow, but there was no significant sign of growth, and the cells began to grow after 24 h. After 36 h, the cells began to grow in the medium containing anthracene, but the medium turned yellow after 48 h. After 72 h, the medium containing fluoranthene turned red and cells began to grow subsequently. After 96 h incubation, strain PYR-1 with all the substrates showed an evident growth (Fig. 2). Strain PYR-1 showed different growth rate with different PAHs, indicating that strain PYR-1 maybe utilize different PAHs with different enzyme systems.

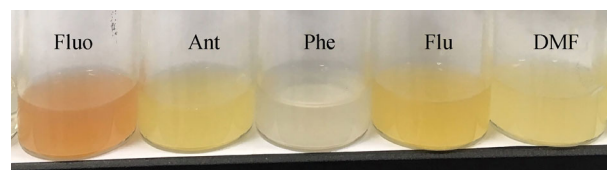


Fig. 2 Growth of *M. vanbaalenii* PYR-1 in the M7H9 medium with PAHs. From left to right represents the growth in the M7H9 medium containing: fluoranthene, anthracene, phenanthrene, fluorene, DMF (*N,N*-Dimethylformamide), respectively.

3.2 NidA3B3 showed activity through co-expression with the endogenous electron transport chain PhtAcAd from a phthalate dioxygenase system

To explore whether the endogenous electron transport chain was compatible with NidA3B3, biotransformation of phenanthrene was conducted by resting cells of strain BL21(DE3) [pNidA3B3-PhtAcAd]. As shown in Fig. 3A, after 5 h incubation, 0.1 mM phenanthrene was almost converted to three corresponding products of *cis*-dihydrodiols detected by GC-MS. It has been reported that there were three sites for phenanthrene to occur dihydroxylation reaction catalyzed by NidA3B3 to form 1, 2-, 3, 4- and 9, 10-dihydrodiols, respectively. All of three peaks have a characteristic ion, m/z 356 [M⁺], which is exactly the molecular weight of *cis*-dihydrodiol-phenanthrene after derivatization. After comparing their mass pattern with reported products, it can be confirmed that these three

peaks are the products of *cis*-dihydrodiol-phenanthrene. According to the ratio of m/z 147 [M^+] and m/z 191 [M^+], the site where the dihydroxylation reaction occurs can be roughly determined: it occurred at K region, the sites 9 and 10, when the ratio was larger than 1 (Zink and Lorber, 1995), so the peak at 19.05 min was *cis*-9, 10-dihydrodiol-phenanthrene (Fig. 3B). It has reported that the major product was *cis*-3,4-dihydrodiol-phenanthrene and the yield of *cis*-1,2-dihydrodiol-phenanthrene is less than 20%, so the peak at 19.99 min was *cis*-3,4-dihydrodiol-phenanthrene (Fig. 3C) and the peak at 20.63 min was *cis*-1,2-dihydrodiol-phenanthrene (Fig. 3D). The order of retention time of the peaks was also consistent with the previously reported results. From the above, it was confirmed that the electron transport chain of the phthalate dioxygenase, PhtAcAd, was compatible with NidA3B3 for catalyzing the dihydroxylation of phenanthrene. Therefore, it was assumed that NidA3B3 maybe share the electron transport chain components of the phthalate dioxygenase PhtAaAbAcAd to catalyze PAHs hydroxylation in vivo.

3.3 The endogenous electron transport chain PhtAcAd endowed an enhanced activity with NidA3B3 compared with PhdCD

As mentioned above, the activity of NidA3B3 was detected by coexpression with the endogenous electron transport chain PhtAcAd, rather than the previously reported exogenous electron transport chain PhdCD. To evaluate the compatibility of these two electron transport chains, biotransformation of phenanthrene by resting cells of *E. coli* BL21(DE3) harboring pNidA3B3-PhtAcAd or pNidA3B3-PhdCD was conducted, and the substrate consumption was analyzed by GC-MS. As shown in Table 3, within 3 h, 25 μ M phenanthrene was entirely consumed by strain BL21(DE3) [pNidA3B3-PhtAcAd], thus the specific activity of biotransformation was calculated as 0.15 ± 0.03 U/mg, but the specific activity of strain BL21(DE3) [pNidA3B3-PhdCD] was only 0.025 ± 0.006 U/mg. The activity of NidA3B3 increased 5 times when equipped with PhtAcAd, compared to

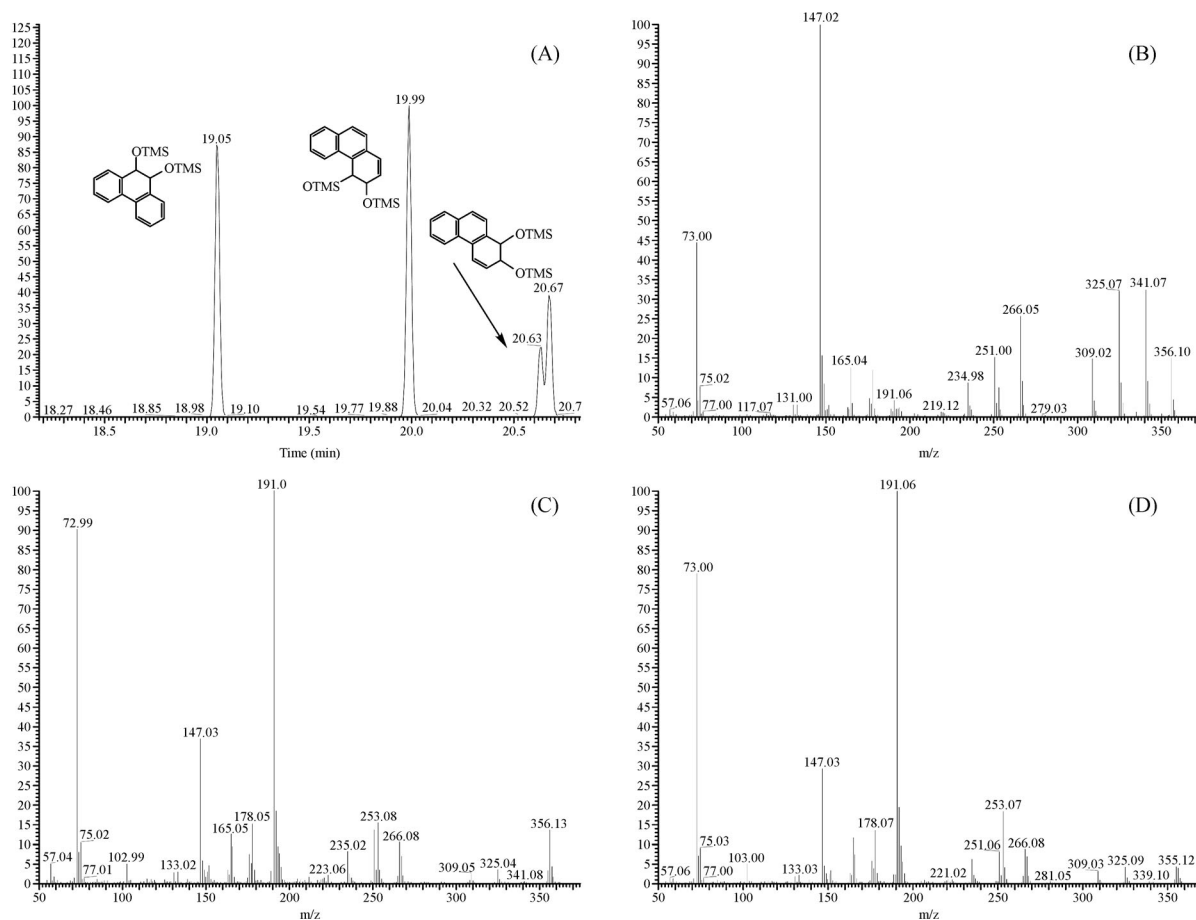


Fig. 3 GC-MS analysis of products from the phenanthrene biotransformation. (A) Extracted ion chromatograms of derivatized products, m/z 356 [M^+]; the reaction yielded 3 products in total; (B) MS of the peak of *cis*-9, 10-dihydrodiol-phenanthrene at 19.05 min; (C) MS of the peak of *cis*-3, 4-dihydrodiol-phenanthrene at 19.99 min; (D) MS of the peak of *cis*-1,2-dihydrodiol-phenanthrene at 20.63 min.

Table 3 Activity comparison of compatibility of electron transport chain PhtAcAd and PhdCD with NidA3B3

Electron transport chain	Specific activity ^{a)} (U/mg)	Relative activity ^{b)} (%)
PhtAcAd	0.15±0.03	100
PhdCD	0.025±0.006	16.7±2.3

Notes: a) 1 unit of biotransformation activity was defined as the dry weight of resting cell required to convert 1 nmol phenanthrene per minute; b) The production by NidA3B3-PhtAcAd was set as 100%.

PhdCD. Therefore, the endogenous electron transport chain components, PhtAcAd were more compatible with the PAHs-ring-hydroxylating dioxygenase, NidA3B3. This significant improvement of catalytic activity provided a great convenience for further study of this type of dioxygenase due to their relatively low activities and the instability of the products formed.

3.4 FNidA3B3 showed an enhanced activity compared with NidA3B3

Basing on genome mining, a new protein FNidA3 encoded by a newly defined ORF was discovered, which had a prolonged 19-amino acid sequence at its N-terminus compared with NidA3. It was unknown about the exact function of these “additional” residues in strain PYR-1. To demonstrate whether the existence of these 19 amino acids could affect its activity, phenanthrene biotransformation was conducted using the resting cells of *E. coli* strains BL21(DE3) [pFNidA3B3-PhtAcAd] and BL21(DE3) [pNidA3B3-PhtAcAd]. As shown in Fig. 4, the catalytic

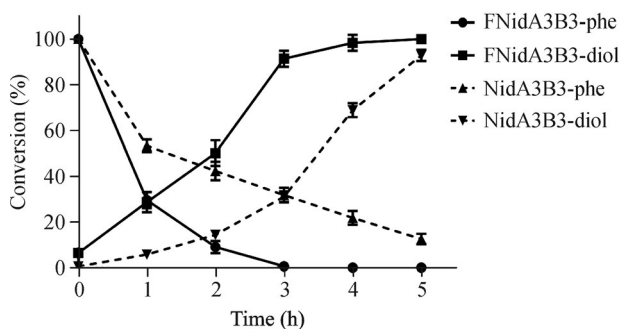


Fig. 4 Time course of biotransformation of phenanthrene. The initial phenanthrene was set 100%; the final dihydrodiol produced by strain BL21(DE3) [pFNidA3B3-PhtAcAd] was set 100%. The sphere in solid line represents phenanthrene consumption by strain BL21(DE3) [pFNidA3B3-PhtAcAd], the square in solid line represents dihydrodiols production by strain BL21(DE3) [pFNidA3B3-PhtAcAd]; the triangle in dot line represents phenanthrene consumption by strain BL21(DE3) [pNidA3B3-PhtAcAd]; the inverted triangle in dot line represents dihydrodiols production by strain BL21(DE3) [pNidA3B3-PhtAcAd]. FNidA3B3 means strain BL21(DE3) [pFNidA3B3-PhtAcAd]; NidA3B3 means strain BL21(DE3) [pNidA3B3-PhtAcAd].

activity of strain BL21(DE3) [pFNidA3B3-PhtAcAd] was remarkably higher than that of strain BL21(DE3) [pNidA3B3-PhtAcAd]. After 3 h, 25 μ M phenanthrene was entirely converted into dihydrodiols by strain BL21(DE3) [pFNidA3B3-PhtAcAd]. While only about 70% phenanthrene was converted by strain BL21(DE3) [pNidA3B3-PhtAcAd] after 3 h, 10% phenanthrene still remained after 5 h. The “additional” 19 amino acid residues endowed FNidA3B3 with an increased activity by 50% approximately compared with NidA3B3. From these results, it probably indicated that the “additional” 19-amino acid sequence at N-terminus of FNidA3 might undertake a physiologic role in vivo. But unfortunately, being exposed to air, the purified FNidA3B3 (Fig. 5A) coupled with PhdAcAd showed no activities. According to our ongoing experiment, purified FNidA3B3 (Fig. 5A) after concentration was sensitive to oxygen and precipitated soon, so purification procedure should be carried out under anaerobic condition. Another reported Rieske oxygenase from *Mycobacterium* encountered the same problem (Capyk et al., 2009).

3.5 Dynamic analysis of components of the endogenous electron transport chain

As an essential part of the ring-hydroxylating dioxygenase system, the electron transport chain is indispensable to shuttle electrons from NADH to terminal oxygenase to complete a reaction cycle. To characterize the electron transport chain of the FNidA3B3-PhtAcAd system, ferredoxin PhtAc and ferredoxin reductase PhtAd were purified using affinity chromatography (Fig. 5B). PhtAd is a flavoprotein containing a NAD⁺ binding domain, responsible for the reduction of ferredoxin using the reducing equivalents from NADH. After purification and concentration, PhtAd was yellow-green, indicating the existence of FAD. PhtAc appeared notably brown, which was the typical color of iron-sulfur cluster. To maintain the content of FAD, a certain and constant concentration of exogenous FAD was added into the reaction mixtures. Basing on the analysis by UV spectrophotometer, K_m , k_{cat} , k_{cat}/K_m values of PhtAd to reduce the artificial electron acceptor DCPIP were 123 ± 26.9 μ M, 503 ± 49.9 min^{-1} , 4.1 $\mu\text{M}^{-1} \cdot \text{min}^{-1}$, respectively. To test the capability of PhtAc, coupled with PhtAd, to transfer electrons, cytochrome c was used as the acceptor, K_m , k_{cat} , k_{cat}/K_m values were 52.5 ± 9.7 μ M, 3.8 ± 0.19 min^{-1} and 0.07 $\mu\text{M}^{-1} \cdot \text{min}^{-1}$, respectively.

3.6 Phylogenetic analysis of PAHs-ring-hydroxylating dioxygenases

To analyze evolutionary relationship of NidA3/FNidA3 and other PAHs-ring-hydroxylating dioxygenases, a phylogenetic tree was constructed by Mega 5.0 using functionally identified dioxygenases. NahAc from *Pseu-*

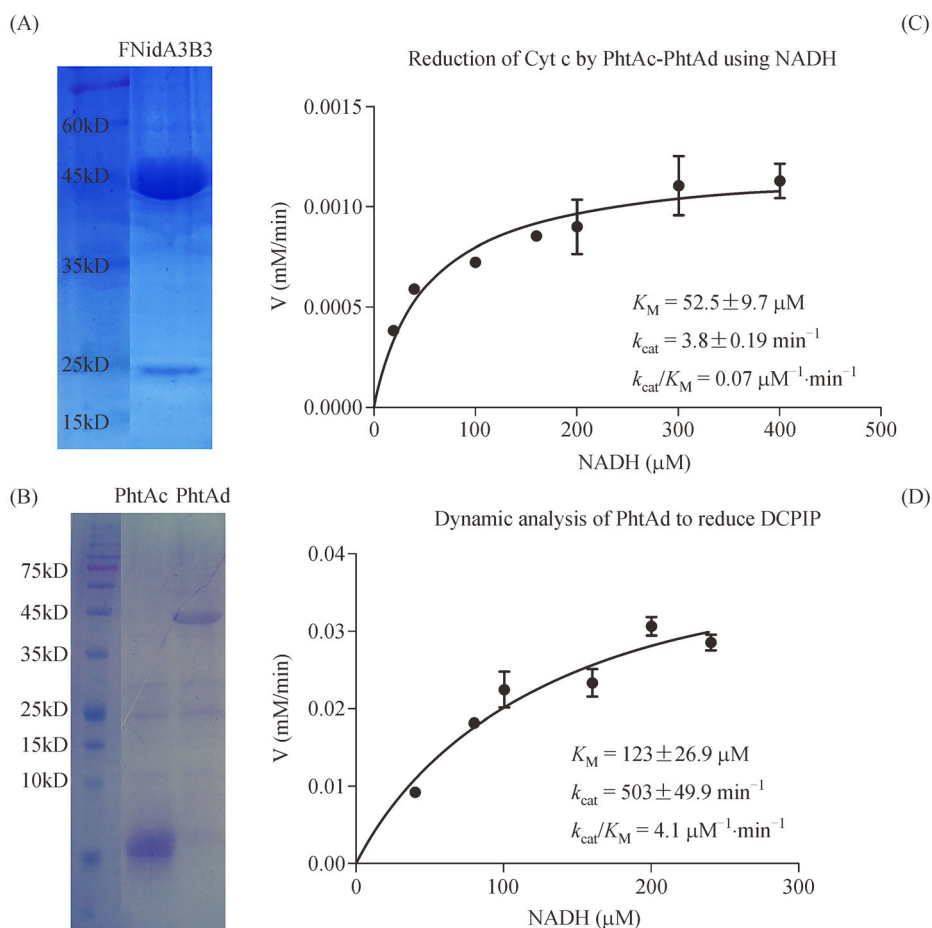


Fig. 5 Enzymatic activities of components of the electron transport chain. (A) SDS-PAGE of the terminal oxygenase, FNidA3B3; (B) SDS-PAGE of components of the electron transport chain, PhtAc and PhtAd; (C) reduction of Cyt c by PhtAc-PhtAd using NADH; (D) dynamic analysis of PhtAd to reduce DCPIP. Cyt c means cytochrome c.

domonas putida NCIMB 9816 (Ensley and Gibson, 1983) and NagAc from *Ralstonia* sp. U2 were classic naphthalene dioxygenases; NarAc from *Rhodococcus* sp. NCIMB 12038 (a Gram positive strain) was also a naphthalene dioxygenase, but showed a relatively high similarity with NidA3 (51% identity of amino acids); BphA1f from *Novosphingobium aromaticivorans* F199 was a biphenyl dioxygenase but exhibited a little activity toward PAHs; PdoA2 from *Mycobacterium* sp. 6PY1 was phenanthrene dioxygenase. As shown in Fig. 6, Phenanthrene dioxygenase PhdA from *Nocardioides* KP7 was near NidA3/FNidA3 in the tree, it explained why NidA3B3 showed activity when equipped with the electron transport chain components from *Nocardioides* KP7. Although NidA shows a moderate similarity (53% at the level of amino acid sequence) with NidA3/FNidA3, they were far away in the phylogenetic tree. NidA was closer toward the dioxygenases from Gram negative strains, which preferred low-molecular-weight PAHs, just as NahAc and NagAc. This meant that they were evolutionarily far apart. In addition, although NidAB and NidA3B3/FNidA3B3 share

a similar substrate specificity, they were regulated in different ways in vivo: NidA was induced by pyrene (Kim et al., 2007) whereas NidA3/FNidA3 remained constant when strain PYR-1 was incubated in fluoranthene (Kweon et al., 2007). This strongly suggested that NidAB and NidA3B3/FNidA3B3 actually represent two different metabolic pathways to degrade PAHs and come from different ancestors even though they utilized a similar range of substrates.

4 Discussion

Ring-hydroxylating reaction is the most important step for soil microorganisms to degrade aromatic hydrocarbon in the environment. There were plenty of reports about this non-heme, iron-dependent dioxygenases and their crystal structures, including dioxygenases of naphthalene, toluene and biphenyl except for PAHs. Most reported degraders of HMW PAHs were clustered in *Mycobacterium*, and it was reported that the horizontal transfer of genes involved in

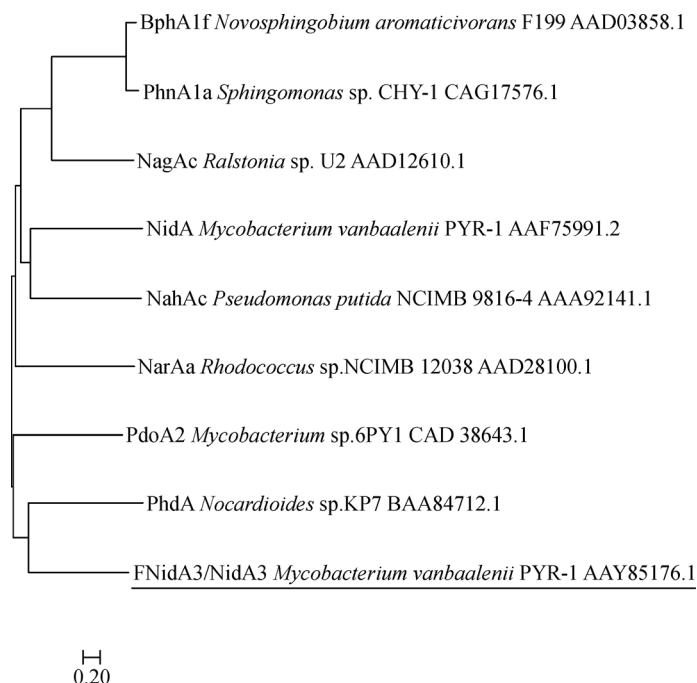


Fig. 6 Phylogenetic analysis of functionally validated PAHs-ring-hydroxylating dioxygenases.

PAHs degradation occurred in this genus (DeBruyn et al., 2012). But no successful purification of ring-hydroxylating dioxygenase specifically favoring HMW PAHs has been reported. There may be some obstacles remaining to be solved, including instability of purified enzymes, their low activity and difficulty of products detection.

A complete phthalate dioxygenase system (Stingley et al., 2004), consisting of both electron transport chain component genes *phtAcAd* and terminal oxygenase genes *phtAaAb*, were found near *nidA3B3* after the genome of strain Pyr-1 was sequenced (Kim et al., 2008). According to the phylogenetic classification system (Kweon et al., 2010), this phthalate dioxygenase and NidA3B3 both belonged to the type V of ring-hydroxylating dioxygenases, in which reductase is glutathione type and ferredoxin is 3Fe-4S type. Therefore, it was assumed that the PAH-ring-hydroxylating dioxygenase NidA3B3 maybe share the electron transport chain components PhtAcAd with the phthalate dioxygenase PhtAaAbAcAd from the same strain. Here, we have largely improved the biotransformation activity of ring-hydroxylating dioxygenases for HMW PAHs, by employing the endogenous electron transport chain and newly defined gene that encoded a larger terminal oxygenase. Indeed, the phenomenon that several dioxygenases shared a single set of electron transport chain was reported two decades ago (Zhou et al., 2002). In this study, the endogenous electron transport chain, PhtAcAd, was more compatible with FNidA3B3/NidA3B3 and significantly enhanced the activity. This result largely facilitated our further research for purified enzymes.

During the purification procedure, we found that cells of strain BL21(DE3) [pFNidA3B3] was becoming relatively easier to be disrupted than strain BL21(DE3) [pNidA3B3] by ultrasonication. It is likely the elevated solubility for the former was one of the reasons for its increased activity. Basing on bioinformatics analysis, several putative NidA3 dioxygenases from other strains of *Mycobacteria* shared 99% identity with FNidA3. All of these putative dioxygenases contained the “additional” 19 amino acid residues at the N-terminus, which indicates that these genes are probably inherited from a same ancestor. Among the 19 amino acid residues, the first 8 amino acid residues were hydrophobic and the last 11 amino acids were hydrophilic. A motif contained 8 conserved amino acid residues (LGAQXXRKVR) in the 19 amino acid residues exists in the phosphotransferase system (PTS) of *Vibrio* (Siebold et al., 2001). And this motif rightly stretches over the hydrophobic area and the hydrophilic area of the 19 amino acid residues. A similar phenomenon was reported in other *Mycobacterium* strains in which several amino acid residues at the N-terminus of a specific protein led to an increase of enzymatic activity (Lama et al., 2009). Just like NO dioxygenase HbN, a type of hemoglobin from *Mycobacterium*, performed better to eliminate NO when it was attached with an “additional” sequence at the N-terminus. This sequence located outside the overall structure of HbN, but could alter the structure of enzyme so that NO is more accessible to the active site. (Lama et al., 2009).

According to phylogenetic analysis, different types of PAHs-ring-hydroxylating dioxygenases have distinct ori-

gins. The dioxygenases preferring HMW PAHs cluster in Gram positive bacteria, including *Mycobacterium*, *Rhodococcus*, *Nocardioide*s; and the dioxygenases for LMW PAHs mostly came from Gram negative bacteria including *Pseudomonas*, *Sphingomonas* (Zhou et al., 2006). Those LMW PAHs degraders have been extensively and profoundly studied, especially the naphthalene dioxygenase NahAc from *P. putida* NCIB 9816-4 (Wolfe et al., 2001; Karlsson et al., 2003) and NagAc from *Ralstonia* sp. U2 (Zhou et al., 2002). Some other dioxygenases, such as biphenyl dioxygenase BphA1f from *Sphingobium yanokuyae* B1, also showed certain activity toward PAHs, even toward those HMW PAHs although at a lower activity (Yu et al., 2007). But up to now, no dioxygenases specifically favoring HMW PAHs have been studied under the level of purified proteins, probably due to their instability and low activity. This problem awaits being solved.

5 Conclusions

In this study, the activity of PAHs-ring-hydroxylating dioxygenase FNidA3B3/NidA3B3 was increased 5 times by employing the endogenous electron transport chain PhtAcAd instead of the exogenous PhdCD. FNidA3, an alpha-subunit of dioxygenase encoded by a newly defined ORF, has a prolonged 19-amino acid sequence at the N-terminus compared with NidA3. With PhtAcAd, FNidA3B3 was endowed with an increased activity by 50% approximately compared with NidA3B3 by biotransformation, probably because these residues increased the solubility of the enzyme, and even altered the structure of the enzyme. The endogenous electron transport chain components PhtAc and PhtAd were purified and characterized. Basing on the phylogenetic analysis, isoenzymes NidA3/FNidA3 and NidA from strain PYR-1 are likely to originate from different ancestors. This study will advance our knowledge of enzymes involved in PAHs degradation by microbes, and also provides a new opportunity for us to investigate thoroughly the Rieske non-heme iron-dependent oxygenase in HMW PAHs degradation.

Acknowledgements This work is supported by the National Key R&D Program of China (Grant No. 2018YFC0309800), National Natural Science Foundation of China (Grant No. 31570100) and Shanghai Science and Technology Commission Scientific Research Project (No. 17JC1403300).

References

Barry S M, Challis G L (2013). Mechanism and catalytic diversity of Rieske non-heme iron-dependent oxygenases. *ACS Catalysis*, 3(10): 2362–2370

Boldrin B, Tiehm A, Fritzsche C (1993). Degradation of phenanthrene, fluorene, fluoranthene, and pyrene by a *Mycobacterium* sp. *Applied and Environmental Microbiology*, 59(6): 1927–1930

Boström C E, Gerde P, Hanberg A, Jernström B, Johansson C, Kyrklund T, Rannug A, Törnqvist M, Victorin K, Westerholm R (2002). Cancer risk assessment, indicators, and guidelines for polycyclic aromatic hydrocarbons in the ambient air. *Environmental Health Perspectives*, 110(Suppl 3): 451–488

Capyk J K, D'Angelo I, Strynadka N C, Eltis L D (2009). Characterization of 3-ketosteroid 9-hydroxylase, a Rieske oxygenase in the cholesterol degradation pathway of *Mycobacterium tuberculosis*. *Journal of biological chemistry*, 284(15): 9937–9946

Cébron A, Norini M P, Beguiristain T, Leyval C (2008). Real-Time PCR quantification of PAH-ring hydroxylating dioxygenase (PAH-RHDalpha) genes from Gram positive and Gram negative bacteria in soil and sediment samples. *Journal of Microbiological Methods*, 73(2): 148–159

Dean-Ross D, Cerniglia C E (1996). Degradation of pyrene by *Mycobacterium flavescens*. *Applied Microbiology and Biotechnology*, 46(3): 307–312

DeBruyn J M, Mead T J, Saylor G S (2012). Horizontal transfer of PAH catabolism genes in *Mycobacterium*: evidence from comparative genomics and isolated pyrene-degrading bacteria. *Environmental Science & Technology*, 46(1): 99–106

Ensley B D, Gibson D T (1983). Naphthalene dioxygenase: Purification and properties of a terminal oxygenase component. *Journal of Bacteriology*, 155(2): 505–511

Fischer F, Raimondi D, Aliverti A, Zanetti G (2002). *Mycobacterium tuberculosis* FprA, a novel bacterial NADPH-ferredoxin reductase. *European Journal of Biochemistry*, 269(12): 3005–3013

Heitkamp M A, Franklin W, Cerniglia C E (1988). Microbial metabolism of polycyclic aromatic hydrocarbons: Isolation and characterization of a pyrene-degrading bacterium. *Applied and Environmental Microbiology*, 54(10): 2549–2555

Karlsson A, Parales J V, Parales R E, Gibson D T, Eklund H, Ramaswamy S (2003). Crystal structure of naphthalene dioxygenase: Side-on binding of dioxygen to iron. *Science*, 299(5609): 1039–1042

Khan A A, Wang R F, Cao W W, Doerge D R, Wennerstrom D, Cerniglia C E (2001). Molecular cloning, nucleotide sequence, and expression of genes encoding a polycyclic aromatic ring dioxygenase from *Mycobacterium* sp. strain PYR-1. *Applied and Environmental Microbiology*, 67(8): 3577–3585

Kim S J, Kweon O, Freeman J P, Jones R C, Adjei M D, Jhoo J W, Edmondson R D, Cerniglia C E (2006). Molecular cloning and expression of genes encoding a novel dioxygenase involved in low- and high-molecular-weight polycyclic aromatic hydrocarbon degradation in *Mycobacterium vanbaalenii* PYR-1. *Applied and Environmental Microbiology*, 72(2): 1045–1054

Kim S J, Kweon O, Jones R C, Edmondson R D, Cerniglia C E (2008). Genomic analysis of polycyclic aromatic hydrocarbon degradation in *Mycobacterium vanbaalenii* PYR-1. *Biodegradation*, 19(6): 859–881

Kim S J, Kweon O, Jones R C, Freeman J P, Edmondson R D, Cerniglia C E (2007). Complete and integrated pyrene degradation pathway in *Mycobacterium vanbaalenii* PYR-1 based on systems biology. *Journal of Bacteriology*, 189(2): 464–472

Kweon O, Kim S J, Freeman J P, Song J, Baek S, Cerniglia C E (2010). Substrate specificity and structural characteristics of the novel Rieske nonheme iron aromatic ring-hydroxylating oxygenases NidAB and

- NidA3B3 from *Mycobacterium vanbaalenii* PYR-1. mBio, 1(2): e00135-10
- Kweon O, Kim S J, Holland R D, Chen H, Kim D W, Gao Y, Yu L R, Baek S, Baek D H, Ahn H, Cerniglia C E (2011). Polycyclic aromatic hydrocarbon metabolic network in *Mycobacterium vanbaalenii* PYR-1. Journal of Bacteriology, 193(17): 4326–4337
- Kweon O, Kim S J, Jones R C, Freeman J P, Adjei M D, Edmondson R D, Cerniglia C E (2007). A polyomic approach to elucidate the fluoranthene-degradative pathway in *Mycobacterium vanbaalenii* PYR-1. Journal of Bacteriology, 189(13): 4635–4647
- Kweon O, Kim S J, Kim D W, Kim J M, Kim H L, Ahn Y, Sutherland J B, Cerniglia C E (2014). Pleiotropic and epistatic behavior of a ring-hydroxylating oxygenase system in the polycyclic aromatic hydrocarbon metabolic network from *Mycobacterium vanbaalenii* PYR-1. Journal of Bacteriology, 196(19): 3503–3515
- Lama A, Pawaria S, Bidon-Chanal A, Anand A, Gelpi J L, Arya S, Marti M, Estrin D A, Luque F J, Dikshit K L (2009). Role of Pre-A motif in nitric oxide scavenging by truncated hemoglobin, HbN, of *Mycobacterium tuberculosis*. Journal of biological chemistry, 284(21): 14457–14468
- McLean K, Dunford A, Sabri M, Neeli R, Girvan H, Balding P, Leys D, Seward H, Marshall K, Munro A (2006). CYP121, CYP51 and Associated Redox Systems in *Mycobacterium tuberculosis*: Towards Deconvoluting Enzymology of P450 Systems in a Human Pathogen. London: Portland Press Limited
- Moody J D, Freeman J P, Doerge D R, Cerniglia C E (2001). Degradation of phenanthrene and anthracene by cell suspensions of *Mycobacterium* sp. strain PYR-1. Applied and Environmental Microbiology, 67(4): 1476–1483
- Moody J D, Freeman J P, Fu P P, Cerniglia C E (2004). Degradation of benzo[a]pyrene by *Mycobacterium vanbaalenii* PYR-1. Applied and Environmental Microbiology, 70(1): 340–345
- Saito A, Iwabuchi T, Harayama S (2000). A novel phenanthrene dioxygenase from *Nocardioides* sp. Strain KP7: Expression in *Escherichia coli*. Journal of Bacteriology, 182(8): 2134–2141
- Schneider J, Grosser R, Jayasimhulu K, Xue W, Warshawsky D (1996). Degradation of pyrene, benz[a]anthracene, and benzo[a]pyrene by *Mycobacterium* sp. strain RJGII-135, isolated from a former coal gasification site. Applied and Environmental Microbiology, 62(1): 13–19
- Siebold C, Flükiger K, Beutler R, Erni B (2001). Carbohydrate transporters of the bacterial phosphoenolpyruvate: sugar phosphotransferase system (PTS). FEBS Letters, 504(3): 104–111
- Stingley R L, Brezna B, Khan A A, Cerniglia C E (2004). Novel organization of genes in a phthalate degradation operon of *Mycobacterium vanbaalenii* PYR-1. Microbiology, 150(11): 3749–3761
- Stone E A, Lough G C, Schauer J J, Praveen P, Corrigan C, Ramanathan V (2007). Understanding the origin of black carbon in the atmospheric brown cloud over the Indian Ocean. Journal of Geophysical Research: Atmospheres, 112(D22): D22S23, 1-10
- Wang L, Gao Y Z, Zhao H, Xu Y, Zhou N Y (2019). Biodegradation of 2-bromonitrobenzene by *Pseudomonas stutzeri* ZWLR2–1. International Biodeterioration & Biodegradation, 138: 87–91
- Wolfe M D, Parales J V, Gibson D T, Lipscomb J D (2001). Single turnover chemistry and regulation of O₂ activation by the oxygenase component of naphthalene 1,2-dioxygenase. Journal of biological chemistry, 276(3): 1945–1953
- Xu Y, Zhou N Y (2017). Microbial remediation of aromatics-contaminated soil. Frontiers of Environmental Science & Engineering, 11(2): 1–9
- Yu C L, Liu W, Ferraro D J, Brown E N, Parales J V, Ramaswamy S, Zylstra G J, Gibson D T, Parales R E (2007). Purification, characterization, and crystallization of the components of a biphenyl dioxygenase system from *Sphingobium yanoikuyae* B1. Journal of Industrial Microbiology & Biotechnology, 34(4): 311–324
- Zhang Y, Tao S, Shen H, Ma J (2009). Inhalation exposure to ambient polycyclic aromatic hydrocarbons and lung cancer risk of Chinese population. Proceedings of the National Academy of Sciences of the United States of America, 106(50): 21063–21067
- Zhou H W, Guo C L, Wong Y S, Tam N F Y (2006). Genetic diversity of dioxygenase genes in polycyclic aromatic hydrocarbon-degrading bacteria isolated from mangrove sediments. FEMS Microbiology Letters, 262(2): 148–157
- Zhou N Y, Al-Dulayymi J, Baird M S, Williams P A (2002). Salicylate 5-hydroxylase from *Ralstonia* sp. strain U2: A monooxygenase with close relationships to and shared electron transport proteins with naphthalene dioxygenase. Journal of Bacteriology, 184(6): 1547–1555
- Zink G, Lorber K E (1995). Mass spectral identification of metabolites formed by microbial degradation of polycyclic aromatic hydrocarbons (PAH). Chemosphere, 31(9): 4077–4084